Anomalous diffusion, non-Gaussianity, nonergodicity, and confinement in stochastic-scaled Brownian motion with diffusing diffusivity dynamics

Yongge Li [1], Kheder Suleiman [1] and Yong Xu [1,2,*]

[1] *School of Mathematics and Statistics, Northwestern Polytechnical University, Xi'an 710072, China*

[2] *MOE Key Laboratory for Complexity Science in Aerospace, Northwestern Polytechnical University, Xi'an 710072, China*

(Received 14 July 2023; revised 20 November 2023; accepted 7 December 2023; published 29 January 2024)

Scaled Brownian motions (SBMs) with power-law time-dependent diffusivity have been used to describe various types of anomalous diffusion yet Gaussian observed in granular gases kinetics, turbulent diffusion, and molecules mobility in cells, to name a few. However, some of these systems may exhibit non-Gaussian behavior which can be described by SBM with diffusing diffusivity (DD-SBM). Here, we numerically investigate both free and confined DD-SBM models characterized by fixed or stochastic scaling exponent of time-dependent diffusivity. The effects of distributed scaling exponent, random diffusivity, and confinement are considered. Different regimes of ultraslow diffusion, subdiffusion, normal diffusion, and superdiffusion are observed. In addition, weak ergodic and non-Gaussian behaviors are also detected. These results provide insights into diffusion in time-fluctuating diffusivity landscapes with potential applications to time-dependent temperature systems spreading in heterogeneous environments.

DOI: 10.1103/PhysRevE.109.014139

I. INTRODUCTION

Diffusion and other transport phenomena in physical, biological, and other systems have always been key to other processes such as reactions to name a few, and sometimes controlling such processes is an aim that first requires establishing the dynamics driving these phenomena. This can be achieved by single-particle tracking (SPT) and statistical observables such as mean-squared displacements (MSD) to characterize the recording datasets, as well as building theoretical models that embody the detected characteristic features [1–4]. These models can be applied later to study related processes. However, some of these models may exhibit nonergodic behavior where the ensemble MSD and mean time-averaged mean-squared displacements (TAMSD) (defined in Sec. II B more precisely) are not identical [5–14]. This requires caution when applying theoretical models and knowledge of the exact behavior of their statistical observables [15].

The systematic study of the diffusion processes dates back to 1828 when Robert Brown noticed an erratic motion of pollen granules in water [16]. The basis of the theory of diffusion process was laid by Einstein, Smoluchowski, and Langevin between 1905 and 1908 [2,16]. It has been shown that the thermal motion of the molecules around a small particle (Brownian one) causes the molecules to strike into it and make it move randomly. Experimental contributions by Perrin and Nordlund led to a better understanding of the diffusion of particles. According to these studies it has been established that the Brownian diffusion has two main characteristics: (1) the time evolution of the ensemble of the diffusive particles follows a Gaussian distribution as predicted by Fick's law, (2) the MSD grows linearly over time.

Rapid technological development in particle tracking in biological systems has given insight into these systems and has opened a new outlook in nanoscience and nanotechnology. The analysis of SPT datasets has shown a deviation from the standard Brownian behavior [2,17–20], in which the MSD grows nonlinearly over time [21–24]. Such a phenomenon is known as anomalous diffusion, which can be classified into different types based on the scaling of MSD. The MSD following the power-law form $\langle x^2(t)\rangle \simeq t^\alpha$ with $0 < \alpha < 1$ refers to subdiffusion, while the case $\alpha > 1$ corresponds to superdiffusion. Subdiffusion behavior has been observed in a variety of systems, such as amorphous semiconductors, subsurface aquifers, live cells, lipid bilayer membranes, and artificially crowded systems [15,20,25–46]. The movements in turbulent systems, weakly chaotic systems, and systems that involve active dynamics have shown superdiffusion behavior [47–54]. Besides, ultraslow diffusion with logarithmic scaling of the MSD, $\langle x^2(t)\rangle \simeq \log^\gamma(t)$, has been demonstrated in various systems [6,55–64]. For $\gamma = 4$, it refers to Sinai diffusion [65,66].

The driving dynamics of anomalous diffusion are nonuniversal in which different dynamics can lead to the same behavior. In this context, several stochastic models based on various physical mechanisms have been suggested to describe this phenomenon [6,13,14]. Examples include, continuous time random walk (CTRW) [67,68] with scale-free waiting time, Lévy walks and flights [8,69], fractional Brownian motion (FBM) [70–73], random walk in fractal and comblike structures [74–78], heterogeneous diffusion processes (HDP) with space-dependent diffusivity [79–87], and scaled Brownian motion (SBM) with time-dependent diffusivity [88–96].

Unlike Brownian motion, the shape of the probability density function (PDF) $P(x,t)$ for the particle displacement at the time step is not always Gaussian in the aforementioned stochastic processes. While the FBM and SBM show a

*Corresponding author: hsux3@nwpu.edu.cn

Gaussian-like distribution, the CTRW and HDP have a non-Gaussian distribution. Recently, a new type of non-Brownian diffusion has been reported in the SPT experiments in a number of biological, soft matter, and other complex systems [97–105]. This diffusion type is known as the Brownian yet non-Gaussian diffusion, in which, the MSD grows linearly over time combined with a non-Gaussian PDF [18,106]. The physical mechanism underlying this behavior can be traced back to environmental heterogeneity. Different approaches have been suggested to describe this phenomenon, among which we mention the concept of superstatistics [107,108] and diffusing diffusivity (DD) [109–111]. For superstatistics, an ensemble of different Brownian particles diffuse in different environments with given diffusion coefficients D. In this context, the PDF of the particle displacement reads $P(x,t) = \int_0^\infty P(D)G(x,t)dD$ where $G(x,t)$ is a Gaussian PDF of individual particles and $p(D)$ is the distribution of local diffusivities [18,106]. For example, the function $P(x,t)$ corresponds to the Laplace distribution, if the distribution $p(D)$ has an exponential shape. However, diffusing diffusivity is similar to the first one yet the diffusivity $D(t)$ continuously fluctuates. The main difference between the two approaches is that the superstatistics leads to non-Gaussian PDF for long times while the DD approach shows a crossover between non-Gaussian PDF for short times and Gaussian PDF for long times [9].

The main objective of this paper is to answer the question of how environmental heterogeneity affects the diffusion of ensemble particles governing by fixed or stochastic-scaled Brownian motion. We assume an ensemble of different tracer particles governed by SBM, and each particle diffuses in its own environment with fluctuating instantaneous diffusivity. We analyze the characteristics of the statistical observables MSD, TAMSD, ergodic parameter, distribution of amplitude scatter of TAMSD, and kurtosis parameter under these dynamics with/without confinement. This problem may be relevant to systems with a time-dependent temperature, such as granular gases [91,112–114], which shows long-time subdiffusive, super-diffusive, or ultraslow behaviors with non-Gaussian distribution for particle displacements, that cannot be described by CTRW, HDP, or DD-FBM [115,116].

The rest of the paper is organized as follows. In Sec. II we introduce the DD-SBM model and the physical observables used in the description. The numerical results for MSD, TAMSD, and mean TAMSD for the cases of free and confined diffusion are investigated in Sec. III A and Sec. III B, respectively. In Sec. IV we analyze the ergodicity breaking, amplitude scatter distribution, and kurtosis for different scenarios. Finally, the conclusions are presented in Sec. V.

II. FORMULATION OF THE DD-SBM MODEL AND PHYSICAL OBSERVABLES

A. Model description and main equations

Let us consider one-dimensional moving particles driven by Gaussian white noise $\xi(t)$ with time-dependent diffusivity $D(t) = D_0(D_{\rm off} + t/\tau_0)^{\alpha-1}$ [117–120], and τ_0 represents a characteristic time for the mobility variation. The constant $D_{\rm off}$ is added to avoid a singularity of $D(t)$ at $t = 0$. We here fix $D_{\rm off} = 1$. Such a diffusion coefficient may be related to the temperature H of the bath in which the particles move and the friction coefficient γ according to the relation $D(t) = H(t)/\gamma(t)m$, where $H(t) = H_0(H_{\rm off} + t/\tau_0)^{2\alpha-2}$, $\gamma(t) = \gamma_0(D_{\rm off} + t/\tau_0)^{\alpha-1}$, $H_0 = H(0)$ the initial temperature, and $\gamma_0 = \gamma(0)$ the initial value of the damping coefficient [92]. The magnitude $\psi(t) = (D_{\rm off} + t/\tau_0)^{\alpha-1}$ decreases as the value of τ_0 gets larger, which in turn encodes a slower drop in temperature. The case $\tau_0 = \infty$ implies a constant diffusion $D(t) = D_0$ and constant temperature $H(t) = H_0$, which in turn corresponds to Brownian motion. In this study, two different scenarios of the exponent α, deterministic and random, will be considered. For the case of deterministic exponent, we assume $0 \leqslant \alpha < 2$. This means that the ensemble of particles with constant α and the magnitude $\psi(t)$ increases or decreases over time for $1 < \alpha < 2$ and $0 \leqslant \alpha < 1$, respectively. For the second scenario, the values of random scaling exponent α for every particle will be chosen from the normal distribution $P(\alpha) = (1/\sqrt{2\pi\sigma^2})\exp[(\alpha-\alpha_0)^2/(2\sigma^2)]$ and $0 \leqslant \alpha_0 < 2$.

Here, we consider $D_0(t) = y^2(t)$ a time random function follows a generalized Gamma distribution, which can be generated from the Ornstein-Uhlenbeck (OU) model $dy(t)/dt = -(1/\varepsilon)[y(t) + \eta(t)]$ where $\eta(t)$ is Gaussian white noise and ε is the correlation time.

If $x(t)$ is the position of the particle at time t, then the corresponding random walks under external force $F(x)$ can be described by the following system:

$$\frac{dx(t)}{dt} = F(x) + \sqrt{2D_0(D_{\rm off} + t/\tau_0)^{\alpha-1}}\xi(t), \tag{1}$$

$$D_0(t) = y^2(t), \tag{2}$$

$$\frac{dy(t)}{dt} = -\frac{1}{\varepsilon}y + \frac{1}{\varepsilon}\eta(t). \tag{3}$$

Stochastic processes experience external confinement is of relevance to transport in porous media, molecule motion in confined cells, and diffusion in brain extracellular space [121,122]. Here, we consider the generic case of confinement in harmonic potential $U(x) = \frac{1}{2}k_0x^2$. In this case the corresponding force $F(x) = -\frac{dU}{dx} = -k_0x$ [38,123]. We note that the approach combining the features of both the SBM and DD models is pioneered in Refs. [124–126] and further developed here and, to the best of our knowledge, it has not been considered in the literature before.

B. Definition of the main observables

We investigate the properties of diffusing particles governed by the system (1)–(3) using the concepts of mean-squared displacement and time-averaged mean-squared displacement. The MSD measures the average of the squared particle position over an ensemble of diffusing particles [2,13,127]:

$$\langle x^2(t)\rangle = \int_{-\infty}^{+\infty} x^2P(x,t)dx, \tag{4}$$

where $P(x,t)$ is the probability density function to find the particle at position x at time t, while the TAMSD for a trajectory $x_k(t)$ of the kth particle for a time span T is defined as

follows:

$$\overline{\delta_k^2(\Delta)} = \frac{1}{T-\Delta}\int_0^{T-\Delta}[x_k(t+\Delta)-x_k(t)]^2 dt, \quad (5)$$

where Δ is the lag time. For an ensemble of N diffusing particles, unlike the ensembled MSD, the realizations $\overline{\delta_k^2(\Delta)}$ for each trajectory $x_k(t)$ at every lag time Δ are random and a scatter of magnitudes between different $\overline{\delta_k^2(\Delta)}$ arises. This scatter is not invariant in all diffusion processes. Thus, the statistical characteristics of the realizations $\overline{\delta_k^2(\Delta)}$ are crucial in determining the underlying dynamics of some anomalous diffusion data. These characteristics can be indicated by the following observables. The mean TAMSD $\langle\overline{\delta^2(\Delta)}\rangle$ over the ensemble of independent TAMSD realizations reads as [2]

$$\langle\overline{\delta^2(\Delta)}\rangle = \frac{1}{N}\sum_{k=1}^{N}\overline{\delta_k^2(\Delta)}. \quad (6)$$

If $\langle x^2(t)\rangle = \lim_{\frac{\Delta}{T}\to 0}\langle\overline{\delta^2(\Delta)}\rangle$, then the process is called ergodic. The amplitude scatter around the mean $\langle\overline{\delta^2(\Delta)}\rangle$ can be quantified by the ergodicity-breaking parameter EB [127]:

$$\mathrm{EB} = \lim_{T\to\infty}\mathrm{EB}(\Delta), \quad (7)$$

where $\mathrm{EB}(\Delta) = \langle\zeta^2(\Delta)\rangle - \langle\zeta(\Delta)\rangle^2$ and $\zeta(\Delta) = \overline{\delta^2(\Delta)}/\langle\overline{\delta^2(\Delta)}\rangle$. Besides, it characterizes the irreproducibility of the stochastic process at hand. The other indicator is the probability density function $\phi(\zeta)$ that is used to quantify the deviation of TAMSD between individual trajectories [127]. For ergodic processes, EB approaches zero and $\phi(\zeta)\to\delta(\zeta-1)$ for long measurement times T. One example of the ergodic processes is the classical Brownian motion (BM) for which

$$\mathrm{EB}(\Delta) = \frac{4\Delta}{3T}, \quad (8)$$

and $\mathrm{EB}=0$ as $\Delta/T\to 0$ [13]. This means that Brownian motion is a fully reproducible process at a long measurement time. Besides, the distribution of the amplitude fluctuations at a given lag time Δ for BM approaches a Gaussian distribution for finite T and a δ function when $T\to\infty$ [71,128]. To check whether the time evolution of PDF of the underlying stochastic process has a Gaussian shape or not the kurtosis parameter is often used. Like the ergodicity-breaking parameter EB, its definition is based on moments according to the following form [110,129]:

$$\mathrm{Kurtosis} = \frac{\langle\overline{\delta^4(\Delta)}\rangle}{\langle\overline{\delta^2(\Delta)}\rangle^2}, \quad (9)$$

where $\overline{\delta^4(\Delta)} = \frac{1}{T-\Delta}\int_0^{T-\Delta}[x(t+\Delta)-x(t)]^4 dt$. If the value of the kurtosis equals 3, the distribution is Gaussian. The kurtosis for BM, FBM, and SBM equals 3; however, it deviates from this value for CTRW and HDP [13].

III. RESULTS: MSD AND TAMSD

A. Free DD-SBM

1. The case of fixed scaling exponent of diffusivity

To understand the impact of random diffusivity on SBM we list here some results for SBM with constant $D_0 = D(0)$, the initial diffusion coefficient, and constant exponent scaling α, as obtained in Refs. [89,130]. Generally, for a given fixed D_0 and fixed exponent $\alpha > 0$, at short times $t \ll \tau_0$ the MSD, $\langle x^2(t)\rangle \sim 2D_0 t$, grows linearly, while it scales as $\langle x^2(t)\rangle \propto t^\alpha$ at long times $t \gg \tau_0$ [92]. Namely, SBM exhibits long-time subdiffusion behavior for $0<\alpha<1$, and long-time superdiffusion behavior for $\alpha>1$. For the TAMSD, the expression $\langle\overline{\delta^2(\Delta)}\rangle \simeq 2D_0\Delta$ is obtained for $\Delta \ll T \ll \tau_0$, and the process is ergodic in the limit of short measurement times, while at longer lag times $\tau_0 \ll \Delta \ll T$ the TAMSD depends on the measurement time T, $\langle\overline{\delta^2(\Delta)}\rangle \simeq (2D_0\Delta)/\alpha(T/\tau_0)^{1-\alpha}$, which reflects an aging phenomenon [90,92]. A similar phenomenon has been observed in the subdiffusive CTRW [127]. The long-time scalings of MSD and TAMSD show fundamentally different scalings of (lag) time dependence, and the SBM is weakly nonergodic in this case [131]. For $\alpha=0$, the MSD has long-time logarithmic scaling, $\langle x^2(t)\rangle \simeq \log(t)$, while the mean TAMSD has a mixed power-law-logarithmic scaling $\langle\overline{\delta^2(\Delta)}\rangle \simeq 2D_0\tau_0(T/\Delta)\log(T/\Delta)$ for long lag time measurements [130]. It should be emphasized that the base of the log function is 10 throughout the paper, including the log scales in the figures. Similar to the case $\alpha>0$, the system also shows short-time ergodic behavior, $\langle\overline{\delta^2(\Delta)}\rangle = \langle x^2(t)\rangle \simeq 2D_0\Delta$, for $\alpha=0$ [92].

For unbiased DD-SBM, we consider two cases of initial condition for $y(t)$, equilibrium and nonequilibrium. For the case of equilibrium initial condition, the initial value $y(0)$ of the OU process $y(t)$ is chosen randomly from the distribution $f(y) = \exp(-y^2)/\sqrt{\pi}$. Thus, the process is stationary and the autocorrelation function of the diffusivity is $\langle\sqrt{D_0(t_1)D_0(t_2)}\rangle = \langle y(t_1)y(t_2)\rangle = (1/2\varepsilon)\exp[-(t_1-t_2)/\varepsilon]$. By integrating Eq. (1) for $x(0)=0$, we obtain the expression

$$\begin{aligned}\langle x^2(t)\rangle &= 2\int_0^t\sqrt{\psi(t_1)}dt_1\int_0^t\sqrt{\psi(t_2)}dt_2\langle\sqrt{D_0(t_1)D_0(t_2)}\rangle \\ &\quad\times\langle\xi(t_1)\xi(t_2)\rangle \\ &= 2\int_0^t dt_1\psi(t_1)\langle D_0(t_1)\rangle \\ &= \frac{1}{\varepsilon}\int_0^t dt_1\psi(t_1) \\ &= \frac{\tau_0}{\varepsilon\alpha}((1+t/\tau_0)^\alpha - 1), \end{aligned} \quad (10)$$

where $\psi(t) = (D_{\mathrm{off}} + t/\tau_0)^{(\alpha-1)}$. According to Eq. (5), the TAMSD reads as

$$\begin{aligned}\langle\overline{\delta^2(\Delta)}\rangle &= \frac{1}{T-\Delta}\int_0^{T-\Delta}\langle(x(t+\Delta)-x(t))^2\rangle dt \\ &= \frac{1}{T-\Delta}\int_0^{T-\Delta}[\langle x^2(t+\Delta)\rangle - 2\langle x(t)x(t+\Delta)\rangle \\ &\quad + \langle x^2(t)\rangle]dt, \end{aligned} \quad (11)$$

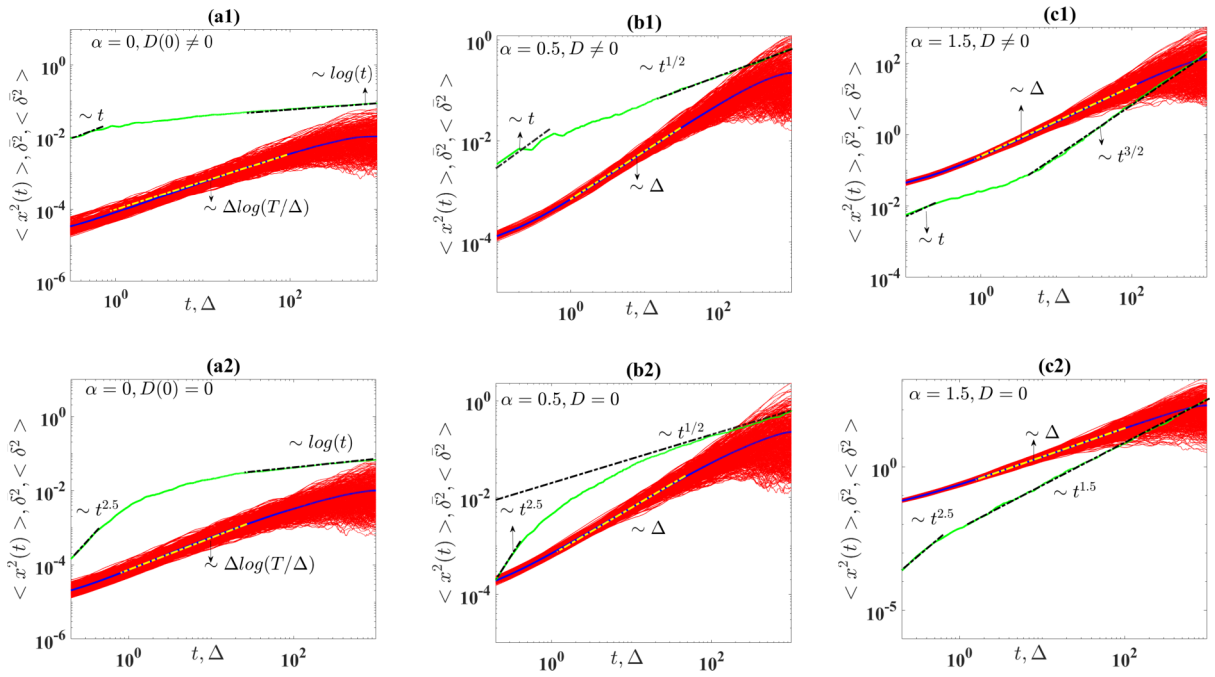

FIG. 1. Ensemble averaged MSD (green "light" gray curves) $\langle x^2(t)\rangle$, TAMSD $\overline{\delta_k^2(\Delta)}$ (thin red curves) of 500 individual trajectories, and mean TAMSD $\langle\overline{\delta^2(\Delta)}\rangle$ (solid blue curves) for unconfined DD-SBM system (1)–(3) with nonequilibrium and equilibrium initial conditions for $y(t)$. The upper panels (a1–c1) correspond to the case of equilibrium initial value which is chosen randomly from the distribution $f(y) = \exp(-y^2)/\sqrt{\pi}$, while the lower panels (a2–c2) refers to the case of nonequilibrium initial condition $D(0) = 0$. The panels are plotted for different values of the fixed scaling exponent α. Other parameters: $\tau_0 = 1$, $\varepsilon = 1$, and $D_{\rm off} = 1$. The total measurement time for the TAMSD is $T = 10^3$.

where

$$\langle x(t)x(t+\Delta)\rangle = \int_0^t \sqrt{\psi(t_1)}dt_1 \int_0^{t+\Delta} \sqrt{\psi(t_2)}dt_2 \times \langle\sqrt{D_0(t_1)D_0(t_2)}\rangle\langle\xi(t_1)\xi(t_2)\rangle = \frac{\tau_0}{\varepsilon\alpha}\left[\left(1+\frac{t}{\tau_0}\right)^{\alpha} - 1\right], \tag{12}$$

which in turn implies that

$$\langle x^2(t+\Delta)\rangle - 2\langle x(t)x(t+\Delta)\rangle + \langle x^2(t)\rangle = \frac{\tau_0}{\varepsilon\alpha}\left(1+\frac{t+\Delta}{\tau_0}\right)^{\alpha} - \frac{\tau_0}{\varepsilon\alpha}\left(1+\frac{t}{\tau_0}\right)^{\alpha}. \tag{13}$$

Then the TAMSD reads as

$$\langle\overline{\delta^2(\Delta)}\rangle = \frac{\tau_0}{\varepsilon\alpha(\alpha+1)(T-\Delta)}\left[1+\left(1+\frac{T}{\tau_0}\right)^{\alpha+1} - \left(1+\frac{\Delta}{\tau_0}\right)^{\alpha+1} - \left(1+\frac{T-\Delta}{\tau_0}\right)^{\alpha+1}\right]. \tag{14}$$

Following the same way, the MSD for $\alpha = 0$ has the formula

$$\langle x^2(t)\rangle = \frac{\tau_0}{\varepsilon}\log\left(1+\frac{t}{\tau_0}\right), \tag{15}$$

and

$$\langle\overline{\delta^2(\Delta)}\rangle = \frac{{\tau_0}^2}{\varepsilon(T-\Delta)}\left[\left(1+\frac{T}{\tau_0}\right)\log\left(1+\frac{T}{\tau_0}\right) - \left(1+\frac{\Delta}{\tau_0}\right)\log\left(1+\frac{\Delta}{\tau_0}\right) - \left(1+\frac{T-\Delta}{\tau_0}\right)\log\left(1+\frac{T-\Delta}{\tau_0}\right)\right]. \tag{16}$$

These results are consistent with their correspondings for the SBM [92]; however, their magnitude is significantly affected by the correlation time ε. The corresponding numerical simulations to this case are presented in the upper panels of Fig. 1 for three values of the scaling exponent, $\alpha = 0, 0.5, 1.5$, with small characteristic time, τ_0, equaling 1. The simulation results show consistency with the theoretical results, in which for $\alpha = 0$, $\langle x^2(t)\rangle \propto \log(t)$ and $\langle\overline{\delta^2(\Delta)}\rangle \propto \Delta\log(T/\Delta)$ at long times, while $\langle x^2(t)\rangle \propto t$ and $\langle\overline{\delta^2(\Delta)}\rangle \propto \Delta$ at short times. For $\alpha > 0$, $\langle x^2(t)\rangle \propto t^{\alpha}$ at long times and $\langle x^2(t)\rangle \propto t$ at short times. The mean TAMSD $\langle\overline{\delta^2(\Delta)}\rangle \propto \Delta$ for both short and long times.

For the case of nonequilibrium initial condition for $y(t)$, the short-time dynamics show nonergodic behavior; see the lower panels in Fig. 1. These simulation results show a crossover diffusion, however, the transition time significantly depends on the values of the characteristic time τ_0 and the correlation time ε; see Figs. 2 and 3. In the case of $\varepsilon < \tau_0$, the MSD initially grows with the superdiffusion scaling $\sim t^{2.5}$

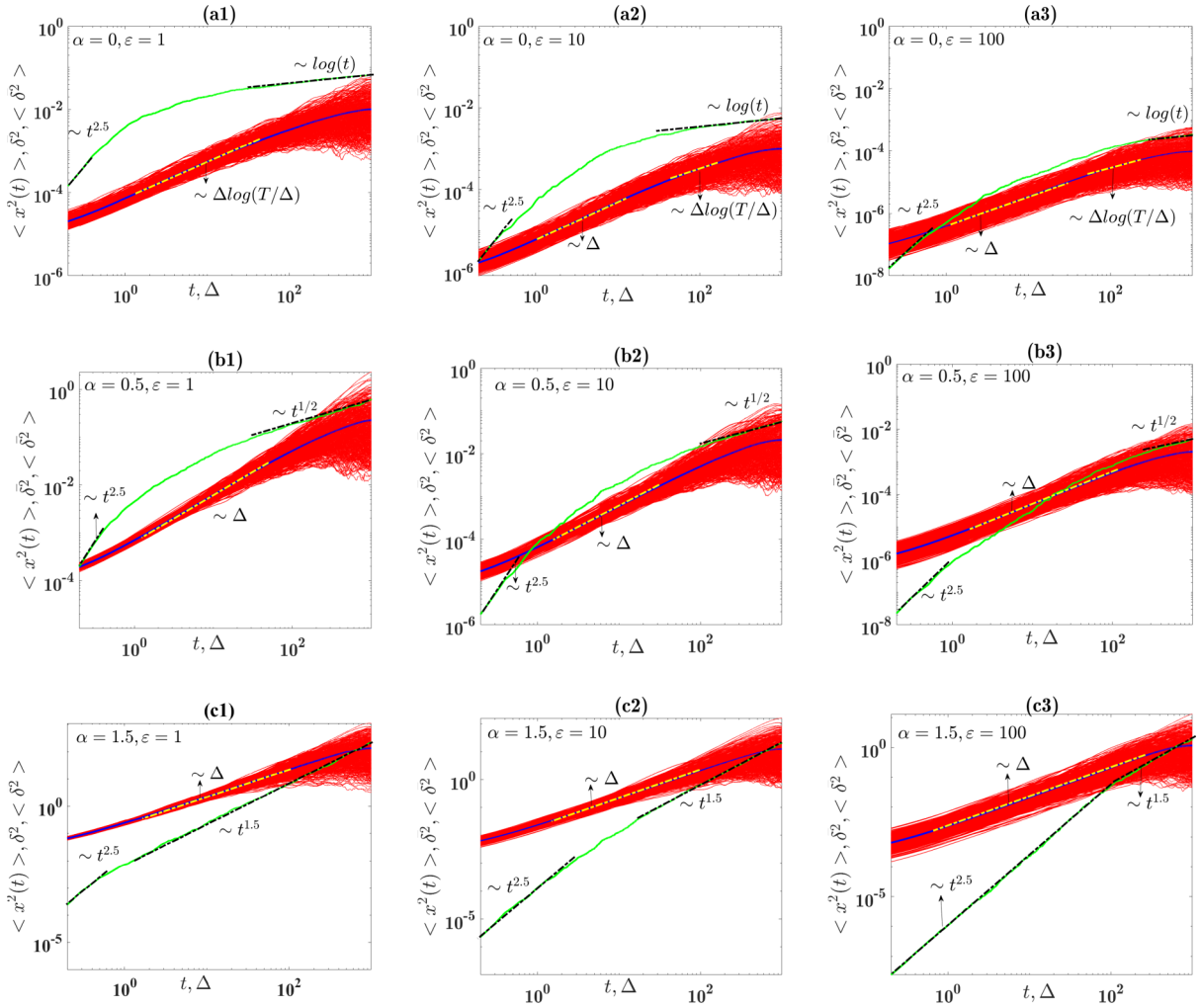

FIG. 2. Ensemble averaged MSD (green "light gray" curves), TAMSD (then red curves) of 500 individual trajectories, and mean TAMSD (solid blue curves) of free diffusive particles subject to DD-SBM dynamics (1)–(3) with fixed exponent α and the correlation time $\varepsilon = 1$ in (a1–c1), $\varepsilon = 10$ in (a2–c2), and $\varepsilon = 100$ in (a3–c3). We chose $\alpha = 0$ in (a1), (a2), and (a3), $\alpha = 0.5$ in (b1), (b2), and (b3), and $\alpha = 1.5$ in (c1), (c2), and (c3). Other parameters: $\tau_0 = 1$ and $D_{\rm off} = 1$. The total measurement time for the TAMSD is $T = 10^3$.

then has the Brownian scaling for $t \ll \tau_0$, and continues with the anomalous diffusion scaling $\sim t^\alpha$ for $\alpha > 0$ and ultraslow diffusion $\sim \log(t)$ for $\alpha = 0$. In the case where the correlation time ε is greater than the characteristic time τ_0, the effects of the nonequilibrium initial condition for diffusivity dominate the behavior of MSD. This shows clearly, especially for the case of $\alpha = 1.5$ in Fig. 2, where the superdiffusion scaling $t^{2.5}$ dominates the MSD for $t < \varepsilon$ before recovering its standard SBM behavior.

For both cases of equilibrium and nonequilibrium initial conditions for diffusivity, specifically, the equilibrium case which is not plotted here, the scatter of TAMSD is significantly affected by ε and τ_0, where the TAMSD trajectories broadly spread as the value of ε gets larger yet the scatter decreases with increasing τ_0. This phenomenon can be attributed to large jumps carried out by some particles from the region of large diffusivity to the region of small diffusivity. These results have been run for a small correlation time ε, which show no influence of the random diffusivity on the standard SBM at long times, except the marginal one for $\alpha = 0$. However, we observe an agreement with the theoretical results for the initial equilibrium conditions of the diffusivity, in which a strong influence on the magnitudes of both MSD and TAMSD for large values of ε. While the characteristic time τ_0 just affects the magnitude of TAMSD. In Fig. 2, for $\alpha = 0$, the magnitude of the TAMSD increases as the value of τ_0 gets larger. However, for $\alpha > 0$, at short times, its effect is almost marginal compared to $\alpha = 0$, however, the long-time behavior is consistent with the theoretical results of standard SBM [92], $\langle \overline{\delta^2(\Delta)} \rangle \sim h(\tau_0) T^\alpha$ and $h(\tau_0) \sim \tau_0^{\alpha-1}$. For $\alpha < 1$ the mean TAMSD is directly proportional to $h(\tau_0)$; otherwise, it is inversely proportional to $h(\tau_0)$.

2. *The case of distributed scaling exponent of diffusivity*

We, here, analyze the dynamics of the unbiased DD-SBM system (1)–(3) with a random α following the normal distribution $P(\alpha) = (1/\sqrt{2\pi\sigma^2}) \exp[(\alpha - \alpha_0)^2/(2\sigma^2)]$. This case may be of relevance to the particle movement with a random power-law-dependent time temperature. Accordingly, the ensemble-averaged MSD, TAMSD, and mean TAMSD for different values of the mean α_0 and varying values of the vari-

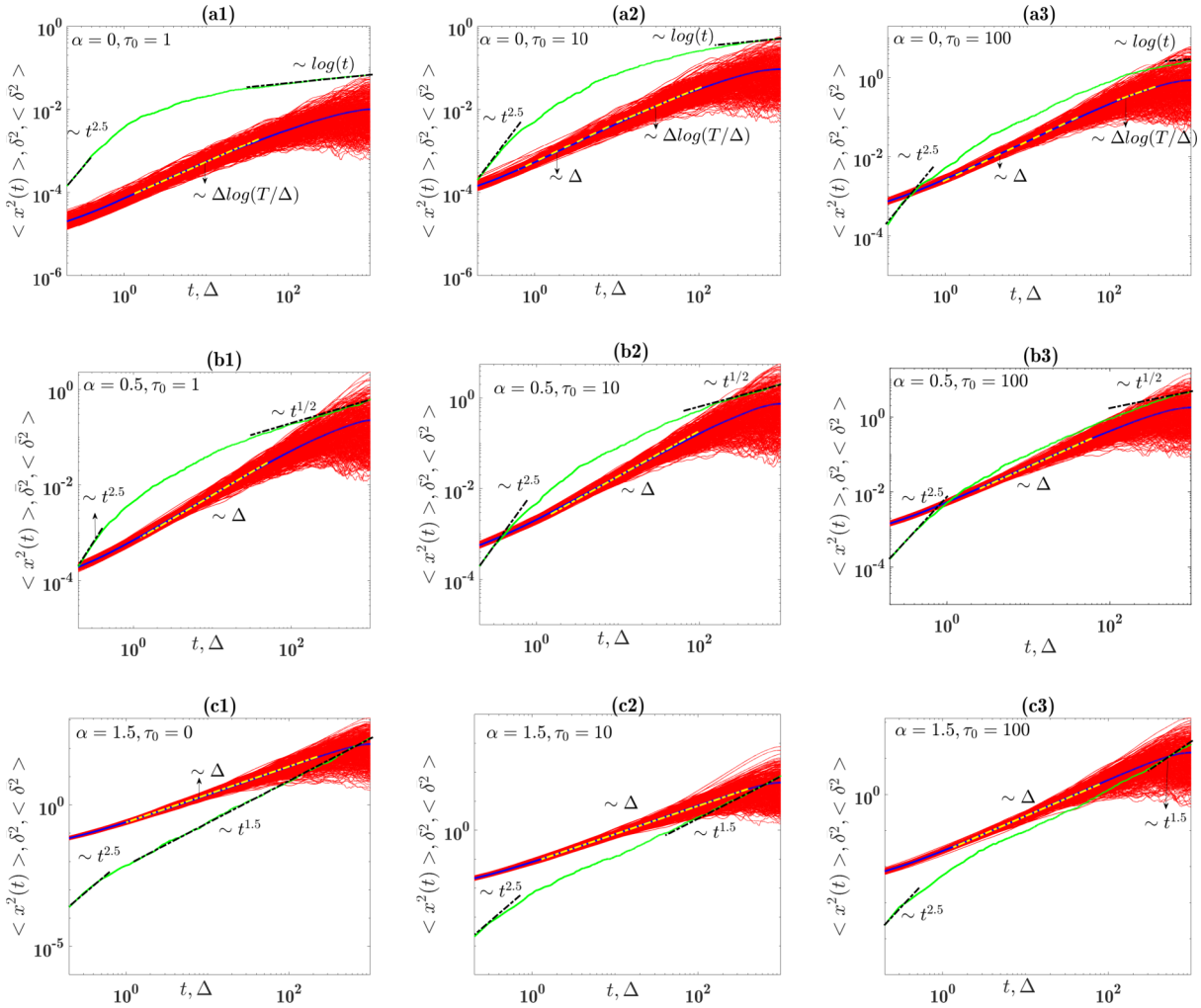

FIG. 3. Ensemble averaged MSD (green "light gray" curves), TAMSD (thin red curves) of 500 individual trajectories, and mean TAMSD (solid blue curves) of free diffusive particles subject to DD-SBM dynamics (1)–(3) with fixed exponent α and the characteristic time $\tau_0 = 1$ in (a1–c1), $\tau_0 = 10$ in (a2–c2), and $\tau_0 = 100$ in (a3–c3). We choose $\alpha = 0$ in (a1), (a2), and (a3), $\alpha = 0.5$ in (b1), (b2), and (b3), and $\alpha = 1.5$ in (c1), (c2), and (c3). Other parameters: $\varepsilon = 1$, and $D_{\rm off} = 1$. The time series length is $T = 10^3$.

ance σ^2 are plotted in Fig. 4. In addition, the initial condition of the diffusivity is considered to be nonequilibrium, while the characteristic time τ_0 and the correlation time ε are chosen to be 1. The results do not show any detectable change from the case of deterministic α exponent, where the system is still weak and nonergodic at long times.

For all cases with $\alpha_0 > 0$, the long-time behavior of MSD dramatically increases with $\sigma \geqslant 0.2$; see Figs. 4(b3) and 4(c3). For example, for $\alpha_0 = 0.5$ as the fluctuating intensity σ increases the behavior of the ensemble MSD and TAMSD and their magnitudes remain quite similar to the case of small σ. However, the magnitude of the mean TAMSD increases compared to the small σ. Besides, the long-time subdiffusive exponent β increases with σ, in which $\beta = 0.6$ for $\sigma = 0.1$, and $\beta = 0.7$ for $\sigma = 0.2$. Unlike $\alpha_0 = 0$, the scatter of individual TAMSDs grows with σ but the magnitude of the effect is similar to that observed for $\alpha_0 = 0$. Back in relation $D(t) = \frac{H(t)}{m\gamma(t)} = \frac{H_0(D_{\rm off}+t/\tau_0)^{2(\alpha-1)}}{\gamma_0(D_{\rm off}+t/\tau_0)^{\alpha-1}}$, where $m = 1$, the above findings concerning the enhancement of the diffusion for $\sigma \geqslant 0.2$ may be interpreted as follows. For case $\alpha_0 = 0.5$, the diffusivity will be only affected by $D_0 = H_0/\gamma_0$ and damping magnitude $(D_{\rm off} + t/\tau_0)^{\alpha-1}$, and the temperature is constant. In the case of random scaling with $\alpha_0 = 0.5$, the increase of σ implies greater temperature specifically at long times.

B. Confined DD-SBM

In this subsection, we characterize the dynamics of diffusive particles governed by the confined DD-SBM system (1)–(3) with the parameters $\tau_0 = 1$, $\varepsilon = 1$, and $k_0 = 0.1$. Accordingly, the initial condition of the diffusivity is considered nonequilibrium with $D(0) = 0$. For the case of deterministic α scaling, we investigate the behavior of the observables for three different values $\alpha = 0, 0.5, 1.5$, while the random values of α are also chosen from the distribution $P(\alpha) = \exp[(\alpha - \alpha_0)^2/(2\sigma^2)]/\sqrt{2\pi\sigma^2}$ with $\alpha_0 = 0, 0.5, 1.5$ and $\sigma = 0.1$.

First, we outline the results for the confined standard SBM for which the diffusivity has the form $D(t) = D_0(1 + t/\tau_0)^{\alpha-1}$ and D_0 is constant. For $\alpha = 0$ the long-time behavior of MSD scales as $\langle x^2(t)\rangle \sim (D_0\tau_0)/(k_0 t)$ [130]. This result reflects the effects of the temporal decay of the temperature encoded

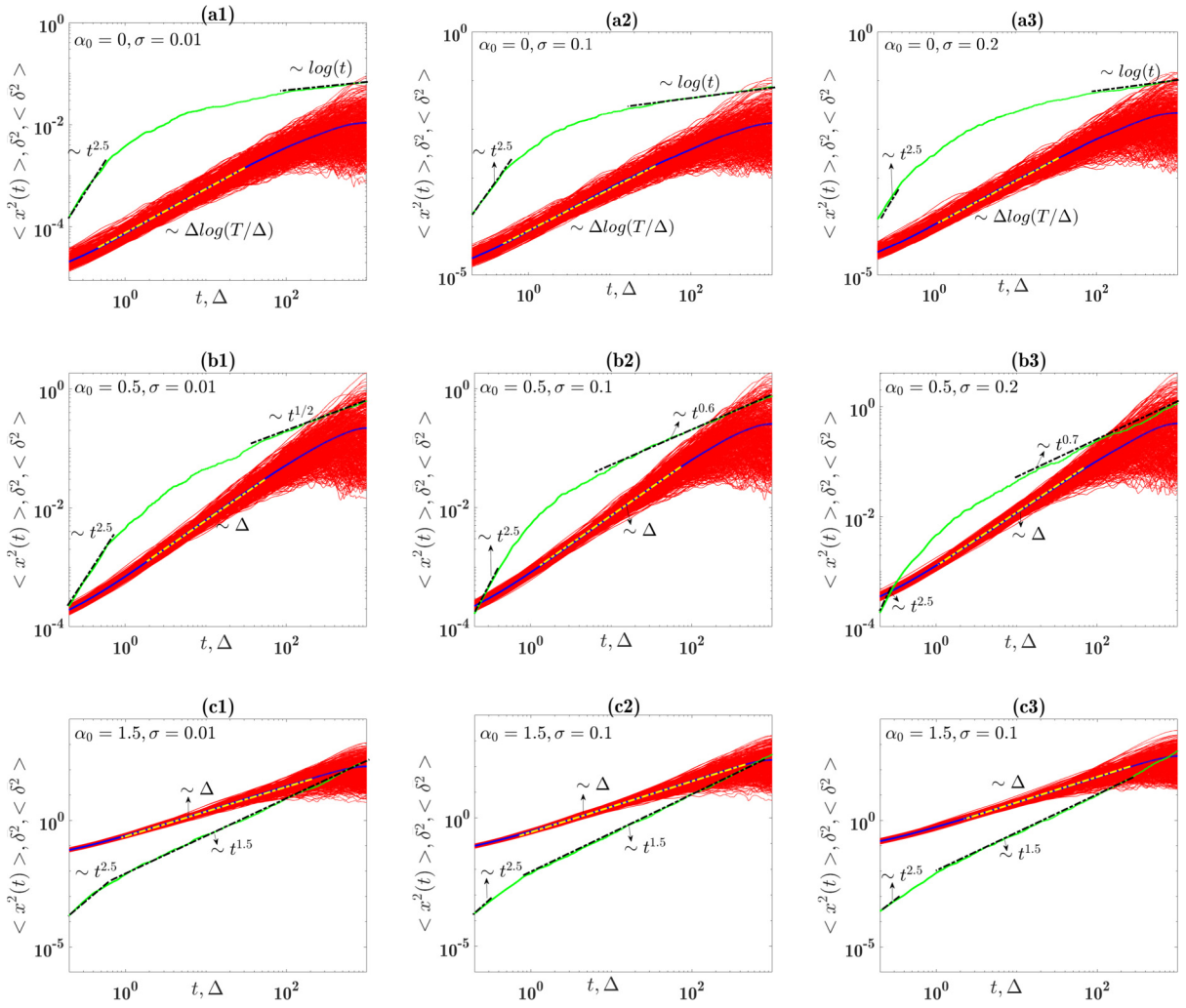

FIG. 4. Ensemble averaged MSD (green "light gray" curves), TAMSD (thin red curves) of 500 individual trajectories, and mean TAMSD (solid blue curves) of free diffusive particles governed by the DD-SBM model (1)–(3) with a random exponent α following normal distribution $P(\alpha) = (1/\sqrt{2\pi\sigma^2})\exp[(\alpha-\alpha_0)^2/(2\sigma^2)]$. $\sigma = 0.01$ in (a1–c1), $\sigma = 0.1$ in (a2–c2), and $\sigma = 0.2$ in (a3–c3). We chose $\alpha_0 = 0$ in (a1), (a2), and (a3), $\alpha_0 = 0.5$ in (b1), (b2), and (b3), and $\alpha_0 = 1.5$ in (c1), (c2), and (c3). Other parameters: $\varepsilon = 1$, $\tau_0 = 1$, and $D_{\text{off}} = 1$. The trajectories length is $T = 10^3$.

in the diffusivity on the confined diffusion dynamics. The long-time behavior of mean TAMSD shows the independence of the lag time and exhibits an apparent plateau $\langle\overline{\delta^2(\Delta)}\rangle \sim 2D_0\tau_0\log(T/\tau_0)/(k_0T)$ [130]. For both $0 < \alpha < 1$ and $\alpha > 1$, the short-time behavior of MSD, $t \ll 1/k_0$, has the scaling form $\langle x^2(t)\rangle \sim t^\alpha$, which fits the long-time behavior for unconfined SBM, while it behaves as $\langle x^2(t)\rangle \sim t^{\alpha-1}$ at long times $t \gg 1/k_0$ [89]. Similar to unconfined SBM for $\alpha > 0$ the short-time behavior of the mean TAMSD grows linearly over lag time Δ, while it has a pronounced plateau at long times. We below report the results of our model.

Figure 5 represents the computer simulation of the MSD, TAMSD, and mean TAMSD for both deterministic and random scaling exponent α. The long-time behaviors of the TAMSD for both cases show an agreement with the theoretical results for the standard confined SBM in which the mean TAMSD has an apparent plateau [89], while it scales as $\Delta^{0.85}$ at short times, except for the case of $\alpha = 0$ in which it has the scaling $\sim\Delta\log(T/\Delta)$. Unlike the lag time independence of the mean TAMSD, the MSD shows a nonstationary behavior at long times for all cases of deterministic and random α, where it has a power-law decay to zero for $\alpha < 1$ and mean $\alpha_0 < 1$ for the case of random scaling, and it grows indefinitely for both $\alpha > 1$ and $\alpha_0 > 1$. These numerical results are consistent with the analytical results for the long-time behavior of MSD for confined standard SBM in which $\langle x^2(t)\rangle \sim t^{\alpha-1}$ [89]. The main difference between confined DD-SBM and confined SBM is the short-time behavior, where the MSD $\langle x^2(t)\rangle$ scales as $t^{5/2}$. In addition, the crossover time of the diffusion regimes for constant α is shorter compared to the random one. Comparing the confined DD-SBM and free DD-SBM dynamics we observe that at short times the diffusive particles subjected to confinement have similar behavior to the long-time behavior of the free diffusive particles before the confinement impact getting emerged.

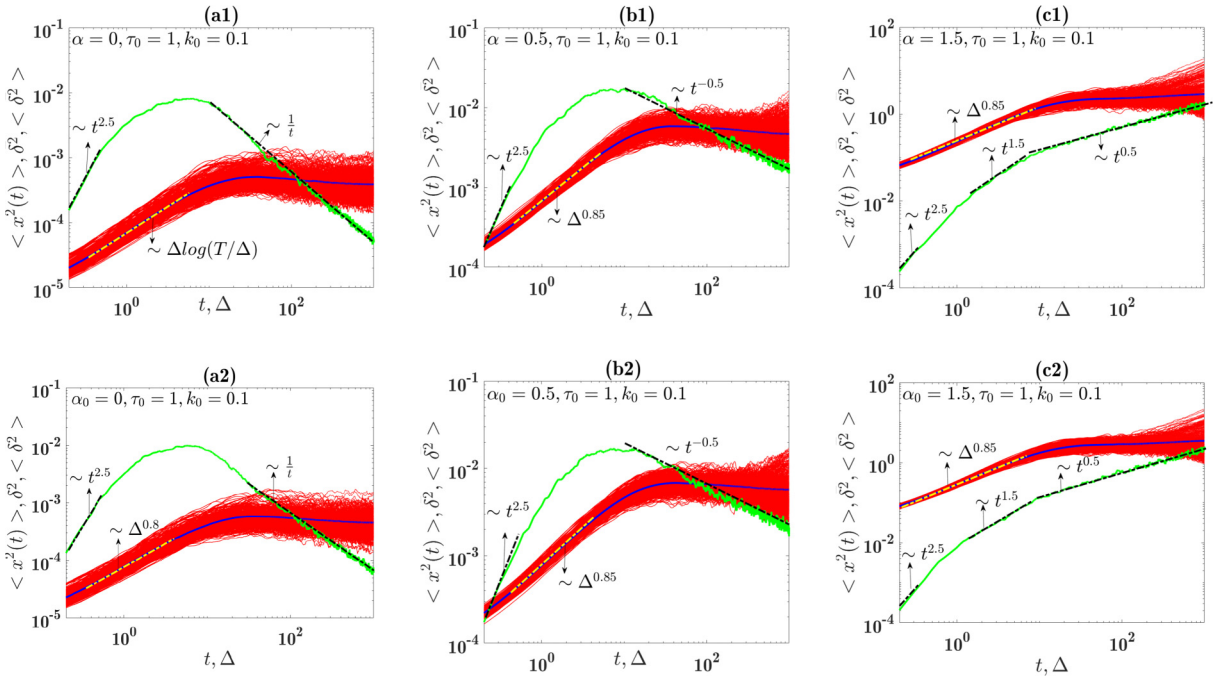

FIG. 5. Ensemble averaged MSD (green "light gray" curves), TAMSD (thin red curves) of 500 individual trajectories, and mean TAMSD (solid blue curves) of confined diffusive particles subject to DD-SBM dynamics (1)–(3). The panels (a1–c1) correspond to the deterministic α case with $\alpha = 0, 0.5, 1.5$, respectively. The panels (a2–c2) correspond to the case of random α with $\alpha_0 = 0, 0.5, 1.5$, respectively. Other parameters: $k_0 = 0.1$, $\sigma = 0.1$, $\varepsilon = 1$, $\tau_0 = 1$, and $D_{\rm off} = 1$. The trajectories length is $T = 10^3$.

IV. ERGODICITY AND NON-GAUSSIANITY

According to the theory, both unconfined FBM and SBM share the same anomalous diffusion behavior and Gaussian PDF; however, SBM exhibits weak nonergodic behavior versus ergodic behavior of the FBM [89,131]. This long-time weak-nonergodic behavior of SBM is also exhibited by CTRW and HDP [13]. The paradox is the ergodicity-breaking parameter EB of SBM decays to zero for sufficiently long times. Moreover, similarly to FBM, the amplitude scatter PDF $\phi(\zeta)$ of individual TAMSD around the mean TAMSD approximates a Gaussian form, yet with a broader width [89]. For ultraslow SBM, $\alpha = 0$, the magnitude EB slowly approaches zero at long measurement times in which $\mathrm{EB}(\Delta) \sim \frac{2.58}{\log^2(T/\Delta)}$ in the period $\tau_0 \ll \Delta \ll T$ [92,130]. For this process, the distribution $\phi(\zeta)$ fits with function $\phi(\zeta) = \exp[-b\zeta - a/\zeta]$. In what follows we will show numerically how these observables behave for the DD-SBM model where the diffusivity has a nonequilibrium initial condition.

A. The ergodicity-breaking variation with lag time measurements

The behaviors of the ergodicity-breaking parameter EB over lag time Δ for both confined and unconfined DD-SBM with deterministic exponent scaling α are sketched in Fig. 6. For unconfined DD-SBM, we observe that $\mathrm{EB} \sim 0.5 \times \ln^{-2}(10^4/\Delta)$ for $\alpha = 0$, $\mathrm{EB} \sim (10^{-4} \times \Delta)^{2\alpha}$ for $0 < \alpha < 0.5$, $\mathrm{EB} \sim 3 \times (10^{-4} \times \Delta) \ln(10^4/\Delta)$ for $\alpha = 0.5$, and $\mathrm{EB} \approx 4 \times 10^{-4}\alpha^2 \times \Delta/3(2\alpha - 1)$ for $\alpha > 0.5$ at $\Delta \ll 10^3$. Besides, when $\Delta = T$ it approaches the value 1 for $\alpha \geqslant 0.5$ and 0.2 for $0 \leqslant \alpha < 0.5$. These observations are consistent with the theory of standard SBM [130,131] in which for the ultraslow regime, $\alpha = 0$, the magnitude EB approaches zero in a logarithmically slow way at large values of T, for the subdiffusion regime $0 < \alpha < 0.5$ it sublinearly tends to zero, while for the subdiffusion regime $0.5 \leqslant \alpha < 1$ and superdiffusion regime $1 < \alpha$ it linearly decays to zero as for Brownian motion $\alpha = 1$. For the confined DD-SBM, at short lag time steps $\Delta \ll 10^2$, similar behavior can be observed except for $\alpha = 0$ in which the magnitude of EB becomes smaller; however, it grows slowly at $\Delta \gg 10^2$. Moreover, due to confinement, it does not approach the value 1 at $\Delta = T$, which is consistent with the fact that at long lag time steps, the magnitudes of TAMSD become more stochastic.

In Fig. 7, we plot the ergodicity-breaking parameter EB over lag time Δ for both confined and unconfined DD-SBM with random α. Comparing Figs. 7 and 6 we do not observe any detectable change in its behavior; however, for $\alpha > 0.5$ its magnitude gets larger and equals to that for $\alpha = 0.5$. In addition, for the unconfined case for $\alpha = 0$ the values of EB get smaller at $\Delta \ll 10^2$, while it does not show any observable change for the confined one.

B. The time evolution of the amplitude scatter

The amplitude fluctuations distribution $\phi(\zeta)$ of individual TAMSD traces for both confined and unconfined DD-SBM with random scaling exponent α for all mean $\alpha_0 = 0$, 0.5, and 1.5 is presented in Fig. 8. For the case of an unconfined DD-SBM system, for both $\alpha_0 = 0.5$ and 1.5 the distribution $\phi(\zeta)$ approximates a Gaussian shape in which its width gets broader as Δ increases. The latter result is consistent with the fact that at long lag time steps, the magnitudes of TAMSD become

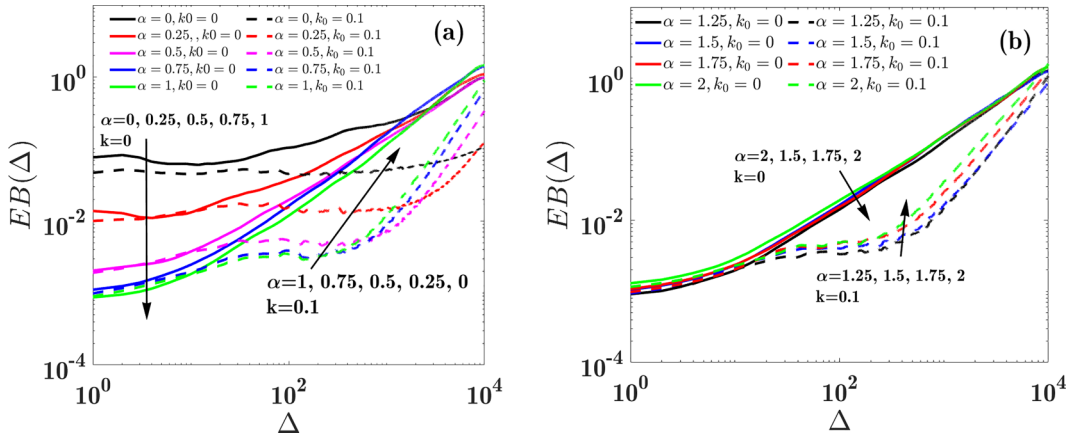

FIG. 6. Variation of ergodic parameter, EB, versus lag time Δ for the values of fixed scaling exponent α given in the legends. The solid and dashed lines correspond to the unconfined and confined process. For confined process, $k_0 = 0.1$. Other parameters $\varepsilon = 1$, $\tau_0 = 1$, and $D_{\text{off}} = 1$.

more stochastic. For $\alpha_0 = 0$ the PDF $\phi(\zeta)$ has an asymmetric right-skewed bell shape. It may be similar to the Gamma distribution observed for the HDP process [79,132] and the function $\phi(\zeta) = \exp[-b\zeta - a/\zeta]$ which is demonstrated for standard SBM [130]. Unlike $\alpha_0 = 0.5$ and 1.5, for $\alpha_0 = 0$ the distribution is broader, and its peak decays slowly which corresponds to the result found in Sec. III B that for $\alpha_0 = 0$ the individual TAMSD trajectories deviate more randomly compared to $\alpha_0 = 0.5$ and 1.5 at short lag time steps. For the confined DD-SBM system, for $\alpha_0 = 0$ there is no detectable change in the shape of the distribution $\phi(\zeta)$, except that it does not evolve over lag time due to confinement, besides, its left tail becomes heavier. Unlike the unconfined case, for $\alpha_0 = 0.5$ and 1.5, we observe that the width of the distribution becomes wider at short lag time steps and slowly evolves over time.

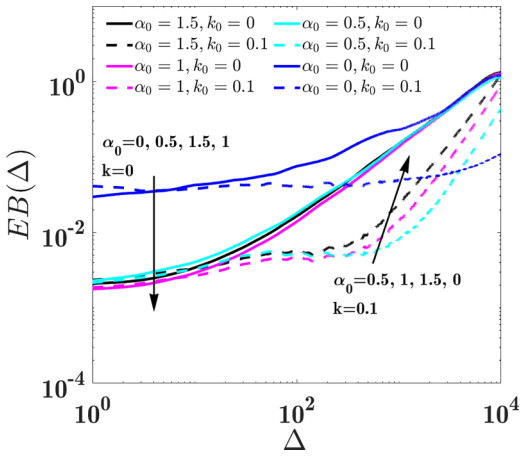

FIG. 7. The parameter EB as a function of lag time Δ, extracted from simulated time series for both unconfined and confined DD-SBM models with stochastic scaling exponent plotted for α. It plots for the values $\alpha_0 = 0.5$, 1, 1.5, with $\sigma = 0.1$. The solid and dashed lines correspond to the unconfined and confined process. For confined process, $k_0 = 0.1$. Other parameters $\varepsilon = 1$, $\tau_0 = 1$, and $D_{\text{off}} = 1$.

C. Kurtosis analysis

In this subsection, we examine the Gaussian nature of the DD-SBM process under different scenarios. So, we extract the kurtosis from the simulated time series of both confined and unconfined DD-SBM models with different fixed α and plot them in Fig. 9. For all $\alpha \neq 1$, we observe that the magnitude of the kurtosis is larger than 3 at short lag time steps; however, it approaches 3 as $\alpha \to 1$ at long lag time measurements $\Delta \gg 10^2$. For $0 \leqslant \alpha < 0.5$, we may conclude that the stochastic process needs large T until it reaches the Gaussian behavior. Unlike the free DD-SBM process, the values of the kurtosis get larger for the confined process and it significantly increases when $0 \leqslant \alpha < 0.5$. For this case, the process shows non-Gaussian behavior even in long-time measurements.

The variations of the kurtosis over lag time for both unconfined and confined DD-SBM with stochastic scaling exponent are presented in Fig. 10. Similar to the previous fixed α case, we find a non-Gaussian behavior of the free DD-SBM process at short lag time steps. However, the values of the kurtosis get smaller and rapidly approach 3 compared to the previous case. For the confined DD-SBM model, the main difference is the magnitudes get smaller, otherwise, the process shows non-Gaussian behavior all the time.

V. CONCLUSION

We have investigated the properties of particle motion governed by DD dynamics combined with SBM. Different scenarios have been considered: confined and unconfined diffusion with fixed and distributed scaling exponent. To quantify the underlying stochastic process of the time series measurement obtained in simulation or experiment, we here focus on studying the behavior of the observables non-Gaussianity (kurtosis), ensemble MSD, and TAMSD, besides the indicators of the individual TAMSD trajectories like mean TAMSD, ergodicity-breaking parameter EB, and the amplitude scatter distribution $\phi(\zeta)$.

We numerically and analytically find that the ensemble MSD, for unconfined DD-SBM systems with fixed scaling exponent and equilibrium initial condition of the diffusivity,

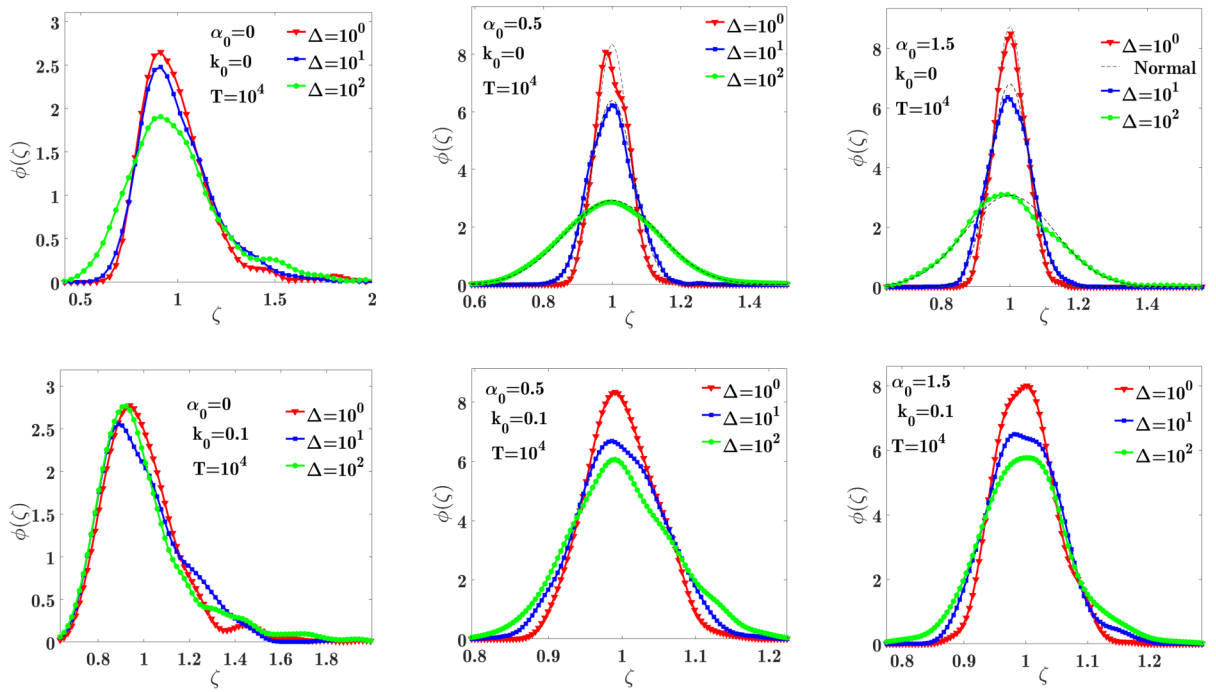

FIG. 8. The amplitude scatter distribution $\phi(\zeta)$ of 500 different individual TAMSD traces extracted from simulated time series for both unconfined and confined DD-SBM models with random exponent α. It plots for the values of $\alpha_0 = 0, 0.5, 1.5$ and lag time steps $\Delta = 10^0, 10^1, 10^2$. The upper and lower panels correspond to the unconfined and confined DD-SBM process, respectively. The dashed line refers to normal distribution. Other parameters: $\varepsilon = 1$, $\tau_0 = 1$, $\sigma = 0.1$, and $D_{\text{off}} = 1$.

characterizes three distinguished crossover diffusion regimes: Brownian diffusion at short times to ultraslow diffusion at long times for $\alpha = 0$, Brownian diffusion at short times to subdiffusion motion at long times for $0 < \alpha < 1$, and Brownian diffusion at short times to superdiffusion motion at long times for $1 < \alpha < 2$. However, the mean TAMSD results show the nonergodic behavior of the considered system, in which it shows a linear growth with lag time Δ for $\alpha > 0$ and sublinear enhanced growth for $\alpha = 0$. These results are somewhat consistent with the SBM's theory [89,92,130,131]. For the nonequilibrium initial condition and for small values of the correlation time ε of the diffusivity, the main difference is that the process shows a crossover from superdiffusion to normal diffusion at short-time measurements. Furthermore, the transition time significantly depends on both the characteristic time τ_0 and correlation time ε, where the effects of the nonequilibrium initial condition for diffusivity dominate the behavior of MSD as ε gets larger. For the case of stochastic scaling exponent α of the diffusivity, we observe that the fluctuating intensity σ of α remarkably affects the magnitude of TAMSD and induces a drop in the initial MSD scaling. Besides, the MSD dramatically increases for all $\alpha > 0$. For confined dynamics, we find that the short-time mean TAMSD scales as $\Delta^{1/2}$ for both fixed and stochastic scaling of the diffusivity. However, it induces an increase for a short time in the MSD scaling. The random diffusivity significantly affects

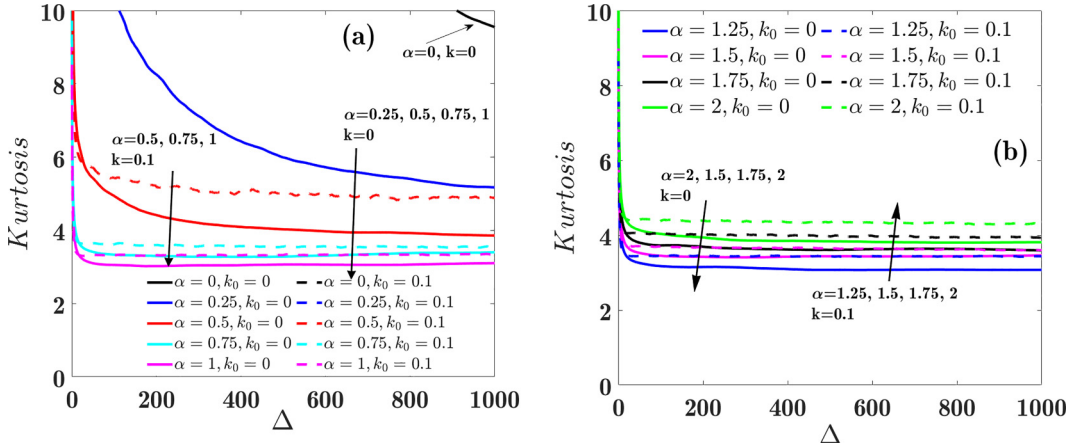

FIG. 9. Variations of kurtosis parameter versus lag time Δ for the values of fixed scaling exponent α given in the legends. The solid dashed lines correspond to the unconfined confined process. For confined process, $k_0 = 0.1$. Other parameters $\varepsilon = 1$, $\tau_0 = 1$, and $D_{\text{off}} = 1$.

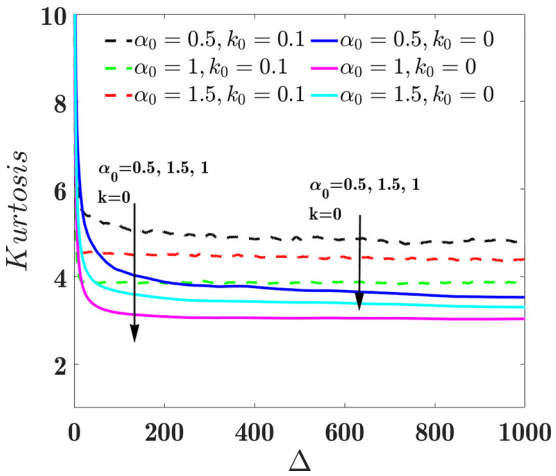

FIG. 10. Kurtosis parameter as a function of lag time Δ, extracted from simulated time series for both unconfined and confined DD-SBM models with stochastic scaling exponent plotted for α. It plots for the values $\alpha_0 = 0.5, 1, 1.5$, with $\sigma = 0.1$. The solid and dashed lines correspond to the unconfined and confined process. For confined process, $k_0 = 0.1$. Other parameters $\varepsilon = 1$, $\tau_0 = 1$, and $D_{\text{off}} = 1$.

the Gaussianity of the SBM process. We find that for all $\alpha \neq 1$ the free DD-SBM has short-time non-Gaussian behavior and long-time Gaussian behavior, however, the convergence speed obviously depends on the value of α in which for $0 \leqslant \alpha < 0.5$, a considerable measurement time T is required to observe the Gaussian phenomenon. For the confined case, the process all the time shows non-Gaussian behavior.

DD-SBM processes reflect the spread of particles governed by SBM law in heterogeneous environments. This process may be relevant to systems with a time-dependent temperature, such as granular gases [91], diffusion on cell surfaces [133], and diffusion in supercooled liquids [119].

ACKNOWLEDGMENTS

This work was partly supported by the NSF of China under Grant No. 12072264 and the Key International (Regional) Joint Research Program of the NSF of China under Grant No. 12120101002. Y.L. thanks the NSF of China for support under Grant No. 12272296, NSF of Chongqing, China for Grant No. cstc2021jcyj-msxmX0738, and NSF of Guangdong Province, China for Grant No. 2023A1515012329.

[1] M. J. Saxton and K. Jacobson, Single-particle tracking: Applications to membrane dynamics, Annu. Rev. Biophys. Biomol. Struct. **26**, 373 (1997).
[2] E. Barkai, Y. Garini, and R. Metzler, Strange kinetics of single molecules in living cells, Phys. Today **65**(8), 29 (2012).
[3] L. E. Sereshki, M. A. Lomholt, and R. Metzler, A solution to the subdiffusion-efficiency paradox: Inactive states enhance reaction efficiency at subdiffusion conditions in living cells, Europhys. Lett. **97**, 20008 (2012).
[4] M. Hellmann, D. W. Heermann, and M. Weiss, Enhancing phosphorylation cascades by anomalous diffusion, Europhys. Lett. **97**, 58004 (2012).
[5] D. Ben-Avraham and S. Havlin, *Diffusion and Reactions in Fractals and Disordered Systems* (Cambridge University Press, Cambridge, UK, 2000).
[6] J.-P. Bouchaud and A. Georges, Anomalous diffusion in disordered media: Statistical mechanisms, models and physical applications, Phys. Rep. **195**, 127 (1990).
[7] Y. Liang, S. Wang, W. Chen, Z. Zhou, and R. L. Magin, A survey of models of ultraslow diffusion in heterogeneous materials, Appl. Mech. Rev. **71**, 040802 (2019).
[8] V. Zaburdaev, S. Denisov, and J. Klafter, Lévy walks, Rev. Mod. Phys. **87**, 483 (2015).
[9] R. Metzler, Superstatistics and non-Gaussian diffusion, Eur. Phys. J.: Spec. Top. **229**, 711 (2020).
[10] S. Havlin and D. Ben-Avraham, Diffusion in disordered media, Adv. Phys. **36**, 695 (1987).
[11] J. W. Haus and K. W. Kehr, Diffusion in regular and disordered lattices, Phys. Rep. **150**, 263 (1987).
[12] F. Höfling and T. Franosch, Anomalous transport in the crowded world of biological cells, Rep. Prog. Phys. **76**, 046602 (2013).
[13] R. Metzler, J. H. Jeon, A. G. Cherstvy, and E. Barkai, Anomalous diffusion models and their properties: Nonstationarity, nonergodicity, and ageing at the centenary of single particle tracking, Phys. Chem. Chem. Phys. **16**, 24128 (2014).
[14] I. M. Sokolov, Models of anomalous diffusion in crowded environments, Soft Matter **8**, 9043 (2012).
[15] Y. Meroz and I. M. Sokolov, A toolbox for determining subdiffusive mechanisms, Phys. Rep. **573**, 1 (2015).
[16] P. Hänggi and F. Marchesoni, Introduction: 100 years of Brownian motion, Chaos **15**, 026101 (2005).
[17] M. F. Shlesinger, G. M. Zaslavsky, and J. Klafter, Strange kinetics, Nature (London) **363**, 31 (1993).
[18] B. Wang, J. Kuo, S. C. Bae, and S. Granick, When Brownian diffusion is not Gaussian, Nat. Mater. **11**, 481 (2012).
[19] R. Metzler, Gaussianity fair: The riddle of anomalous yet non-Gaussian diffusion, Biophys. J. **112**, 413 (2017).
[20] C. Manzo and M. F. Garcia-Parajo, A review of progress in single particle tracking: From methods to biophysical insights, Rep. Prog. Phys. **78**, 124601 (2015).
[21] M. J. Saxton, A biological interpretation of transient anomalous subdiffusion. I. Qualitative model, Biophys. J. **92**, 1178 (2007).
[22] J. Spiechowicz, J. Łuczka, and P. Hänggi, Transient anomalous diffusion in periodic systems: Ergodicity, symmetry breaking and velocity relaxation, Sci. Rep. **6**, 30948. (2016).
[23] M. J. Saxton, Diffusion of dna-binding species in the nucleus: A transient anomalous subdiffusion model, Biophys. J. **118**, 2151 (2020).
[24] M. R. Shaebani and H. Rieger, Transient anomalous diffusion in run-and-tumble dynamics, Front. Phys. **7**, 120 (2019).
[25] K. Burnecki, E. Kepten, J. Janczura, I. Bronshtein, Y. Garini, and A. Weron, Universal algorithm for identification of

fractional Brownian motion: A case of telomere subdiffusion, Biophys. J. **103**, 1839 (2012).
[26] E. Kepten, I. Bronshtein, and Y. Garini, Ergodicity convergence test suggests telomere motion obeys fractional dynamics, Phys. Rev. E **83**, 041919 (2011).
[27] D. Ernst, M. Hellmann, J. Köhler, and M. Weiss, Fractional Brownian motion in crowded fluids, Soft Matter **8**, 4886 (2012).
[28] A. V. Weigel, B. Simon, M. M. Tamkun, and D. Krapf, Ergodic and nonergodic processes coexist in the plasma membrane as observed by single-molecule tracking, Proc. Natl. Acad. Sci. USA **108**, 6438 (2011).
[29] F. Etoc, E. Balloul, C. Vicario, D. Normanno, D. Liße, A. Sittner, J. Piehler, M. Dahan, and M. Coppey, Nonspecific interactions govern cytosolic diffusion of nanosized objects in mammalian cells, Nat. Mater. **17**, 740 (2018).
[30] M. Weiss, M. Elsner, F. Kartberg, and T. Nilsson, Anomalous subdiffusion is a measure for cytoplasmic crowding in living cells, Biophys. J. **87**, 3518 (2004).
[31] M. Woringer, I. Izeddin, C. Favard, and H. Berry, Anomalous subdiffusion in living cells: bridging the gap between experiments and realistic models through collaborative challenges, Front. Phys. **8**, 134 (2020).
[32] S.-L. Liu, Z.-G. Wang, H.-Y. Xie, A.-A. Liu, D. C. Lamb, and D.-W. Pang, Single-virus tracking: from imaging methodologies to virological applications, Chem. Rev. **120**, 1936 (2020).
[33] I. Goychuk, Viscoelastic subdiffusion in a random Gaussian environment, Phys. Chem. Chem. Phys. **20**, 24140 (2018).
[34] P. C. Bressloff and J. M. Newby, Stochastic models of intracellular transport, Rev. Mod. Phys. **85**, 135 (2013).
[35] J.-H. Jeon, Hector Martinez-Seara Monne, M. Javanainen, and R. Metzler, Anomalous diffusion of phospholipids and cholesterols in a lipid bilayer and its origins, Phys. Rev. Lett. **109**, 188103 (2012).
[36] S. Stachura and G. R. Kneller, Communication: Probing anomalous diffusion in frequency space, J. Chem. Phys. **143**, 191103 (2015).
[37] S. C. Weber, A. J. Spakowitz, and J. A. Theriot, Bacterial chromosomal loci move subdiffusively through a viscoelastic cytoplasm, Phys. Rev. Lett. **104**, 238102 (2010).
[38] J.-H. Jeon, V. Tejedor, S. Burov, E. Barkai, C. Selhuber-Unkel, K. Berg-Sørensen, L. Oddershede, and R. Metzler, *In vivo* anomalous diffusion and weak ergodicity breaking of lipid granules, Phys. Rev. Lett. **106**, 048103 (2011).
[39] I. Golding and E. C. Cox, Physical nature of bacterial cytoplasm, Phys. Rev. Lett. **96**, 098102 (2006).
[40] D. Koppel, M. Sheetz, and M. Schindler, Lateral diffusion in biological membranes. a normal-mode analysis of diffusion on a spherical surface, Biophys. J. **30**, 187 (1980).
[41] D. Holcman and Z. Schuss, 100 years after smoluchowski: stochastic processes in cell biology, J. Phys. A: Math. Theor. **50**, 093002 (2017).
[42] F. Xiao, J. Hrabe, and S. Hrabetova, Anomalous extracellular diffusion in rat cerebellum, Biophys. J. **108**, 2384 (2015).
[43] J.-H. Jeon, M. Javanainen, H. Martinez-Seara, R. Metzler, and I. Vattulainen, Protein crowding in lipid bilayers gives rise to non-Gaussian anomalous lateral diffusion of phospholipids and proteins, Phys. Rev. X **6**, 021006 (2016).
[44] R. Metzler, J.-H. Jeon, and A. Cherstvy, Non-Brownian diffusion in lipid membranes: Experiments and simulations, Biochim. Biophys. Acta Biomembr. **1858**, 2451 (2016).
[45] M. Weiss, H. Hashimoto, and T. Nilsson, Anomalous protein diffusion in living cells as seen by fluorescence correlation spectroscopy, Biophys. J. **84**, 4043 (2003).
[46] W. Young, A. Pumir, and Y. Pomeau, Anomalous diffusion of tracer in convection rolls, Phys. Fluids **1**, 462 (1989).
[47] J. F. Reverey, J.-H. Jeon, H. Bao, M. Leippe, R. Metzler, and C. Selhuber-Unkel, Superdiffusion dominates intracellular particle motion in the supercrowded cytoplasm of pathogenic *Acanthamoeba castellanii*, Sci. Rep. **5**, 11690 (2015).
[48] A. Caspi, R. Granek, and M. Elbaum, Enhanced diffusion in active intracellular transport, Phys. Rev. Lett. **85**, 5655 (2000).
[49] N. Gal and D. Weihs, Experimental evidence of strong anomalous diffusion in living cells, Phys. Rev. E **81**, 020903(R) (2010).
[50] T. Komorowski and S. Olla, On the superdiffusive behavior of passive tracer with a Gaussian drift, J. Stat. Phys. **108**, 647 (2002).
[51] J.-P. Bouchaud, A. Georges, J. Koplik, A. Provata, and S. Redner, Superdiffusion in random velocity fields, Phys. Rev. Lett. **64**, 2503 (1990).
[52] N. E. Humphries, H. Weimerskirch, N. Queiroz, E. J. Southall, and D. W. Sims, Foraging success of biological Lévy flights recorded in situ, Proc. Natl. Acad. Sci. USA **109**, 7169 (2012).
[53] T. H. Solomon, E. R. Weeks, and H. L. Swinney, Observation of anomalous diffusion and Lévy flights in a two-dimensional rotating flow, Phys. Rev. Lett. **71**, 3975 (1993).
[54] G. Ariel, A. Rabani, S. Benisty, J. D. Partridge, R. M. Harshey, and A. Be'Er, Swarming bacteria migrate by Lévy walk, Nat. Commun. **6**, 8396 (2015).
[55] M. A. Lomholt, L. Lizana, R. Metzler, and T. Ambjörnsson, Microscopic origin of the logarithmic time evolution of aging processes in complex systems, Phys. Rev. Lett. **110**, 208301 (2013).
[56] L. P. Sanders, M. A. Lomholt, L. Lizana, K. Fogelmark, R. Metzler, and T. Ambjörnsson, Severe slowing-down and universality of the dynamics in disordered interacting many-body systems: Ageing and ultraslow diffusion, New J. Phys. **16**, 113050 (2014).
[57] O. Bénichou and G. Oshanin, Ultraslow vacancy-mediated tracer diffusion in two dimensions: The Einstein relation verified, Phys. Rev. E **66**, 031101 (2002).
[58] S. De Toro Arias, X. Waintal, and J.-L. Pichard, Two interacting particles in a disordered chain III: Dynamical aspects of the interplay disorder-interaction, Eur. Phys. J. B **10**, 149 (1999).
[59] F. Iglói, L. Turban, and H. Rieger, Anomalous diffusion in aperiodic environments, Phys. Rev. E **59**, 1465 (1999).
[60] D. S. Dean, S. Gupta, G. Oshanin, A. Rosso, and G. Schehr, Diffusion in periodic, correlated random forcing landscapes, J. Phys. A: Math. Theor. **47**, 372001 (2014).
[61] P. Le Doussal, C. Monthus, and D. S. Fisher, Random walkers in one-dimensional random environments: Exact renormalization group analysis, Phys. Rev. E **59**, 4795 (1999).
[62] D. S. Fisher, P. Le Doussal, and C. Monthus, Nonequilibrium dynamics of random field ising spin chains: Exact results via

real space renormalization group, Phys. Rev. E **64**, 066107 (2001).
[63] J. Dräger and J. Klafter, Strong anomaly in diffusion generated by iterated maps, Phys. Rev. Lett. **84**, 5998 (2000).
[64] M. Sperl, Nearly logarithmic decay in the colloidal hard-sphere system, Phys. Rev. E **71**, 060401(R) (2005).
[65] Y. G. Sinai, The limiting behavior of a one-dimensional random walk in a random medium, Theory Probab. Appl. **27**, 256 (1983).
[66] G. Oshanin, A. Rosso, and G. Schehr, Anomalous fluctuations of currents in sinai-type random chains with strongly correlated disorder, Phys. Rev. Lett. **110**, 100602 (2013).
[67] J. Klafter and I. M. Sokolov, *First Steps in Random Walks: From Tools to Applications* (Oxford University Press, Oxford, UK, 2011).
[68] R. Metzler and J. Klafter, The random walk's guide to anomalous diffusion: A fractional dynamics approach, Phys. Rep. **339**, 1 (2000).
[69] A. V. Chechkin, V. Y. Gonchar, J. Klafter, and R. Metzler, Fundamentals of Lévy flight processes, in *Fractals, Diffusion, and Relaxation in Disordered Complex Systems: Advances in Chemical Physics, Part B*, edited by W. T. Coffey and Y. P. Kalmykov (John Wiley & Sons, New York, 2006), Chap. 9, pp. 439–496.
[70] E. Lutz, Fractional Langevin equation, Phys. Rev. E **64**, 051106 (2001).
[71] W. Deng and E. Barkai, Ergodic properties of fractional Brownian-Langevin motion, Phys. Rev. E **79**, 011112 (2009).
[72] B. B. Mandelbrot and J. W. Van Ness, Fractional Brownian motions, fractional noises and applications, SIAM Rev. **10**, 422 (1968).
[73] J.-H. Jeon and R. Metzler, Fractional Brownian motion and motion governed by the fractional Langevin equation in confined geometries, Phys. Rev. E **81**, 021103 (2010).
[74] A. Iomin, V. Méndez, and W. Horsthemke, *Fractional Dynamics in Comblike Structures* (World Scientific, Singapore, 2018).
[75] R. Rammal and G. Toulouse, Random walks on fractal structures and percolation clusters, J. Phys. Lett. **44**, 13 (1983).
[76] R. Rammal, Random walk statistics on fractal structures, J. Stat. Phys. **36**, 547 (1984).
[77] S. Havlin, J. E. Kiefer, and G. H. Weiss, Anomalous diffusion on a random comblike structure, Phys. Rev. A **36**, 1403 (1987).
[78] V. Arkhincheev and E. Baskin, Anomalous diffusion and drift in a comb model of percolation clusters, Zh. Eksp. Teor. Fiz. **100**, 292 (1991) [Sov. Phys. JETP **73**, 161 (1991)].
[79] A. G. Cherstvy and R. Metzler, Nonergodicity, fluctuations, and criticality in heterogeneous diffusion processes, Phys. Rev. E **90**, 012134 (2014).
[80] Y. Xu, X. Liu, Y. Li, and R. Metzler, Heterogeneous diffusion processes and nonergodicity with Gaussian colored noise in layered diffusivity landscapes, Phys. Rev. E **102**, 062106 (2020).
[81] A. G. Cherstvy, A. V. Chechkin, and R. Metzler, Anomalous diffusion and ergodicity breaking in heterogeneous diffusion processes, New J. Phys. **15**, 083039 (2013).
[82] N. M. Mutothya, Y. Xu, Y. Li, and R. Metzler, Characterising stochastic motion in heterogeneous media driven by coloured non-Gaussian noise, J. Phys. A: Math. Theor. **54**, 295002 (2021).
[83] T. Sandev, A. Schulz, H. Kantz, and A. Iomin, Heterogeneous diffusion in comb and fractal grid structures, Chaos Solitons Fract. **114**, 551 (2018).
[84] Y. Li, Y. Xu, J. Kurths, and J. Duan, The influences of correlated spatially random perturbations on first passage time in a linear-cubic potential, Chaos **29**, 101102 (2019).
[85] Y. Li, R. Mei, Y. Xu, J. Kurths, J. Duan, and R. Metzler, Particle dynamics and transport enhancement in a confined channel with position-dependent diffusivity, New J. Phys. **22**, 053016 (2020).
[86] D. S. Grebenkov and L. Tupikina, Heterogeneous continuous-time random walks, Phys. Rev. E **97**, 012148 (2018).
[87] W. Wang, A. G. Cherstvy, X. Liu, and R. Metzler, Anomalous diffusion and nonergodicity for heterogeneous diffusion processes with fractional Gaussian noise, Phys. Rev. E **102**, 012146 (2020).
[88] S. C. Lim and S. V. Muniandy, Self-similar Gaussian processes for modeling anomalous diffusion, Phys. Rev. E **66**, 021114 (2002).
[89] J.-H. Jeon, A. V. Chechkin, and R. Metzler, Scaled Brownian motion: A paradoxical process with a time dependent diffusivity for the description of anomalous diffusion, Phys. Chem. Chem. Phys. **16**, 15811 (2014).
[90] H. Safdari, A. V. Chechkin, G. R. Jafari, and R. Metzler, Aging scaled Brownian motion, Phys. Rev. E **91**, 042107 (2015).
[91] A. Bodrova, A. V. Chechkin, A. G. Cherstvy, and R. Metzler, Quantifying non-ergodic dynamics of force-free granular gases, Phys. Chem. Chem. Phys. **17**, 21791 (2015).
[92] A. S. Bodrova, A. V. Chechkin, A. G. Cherstvy, H. Safdari, I. M. Sokolov, and R. Metzler, Underdamped scaled Brownian motion: (Non)existence of the overdamped limit in anomalous diffusion, Sci. Rep. **6**, 30520 (2016).
[93] H. Safdari, A. G. Cherstvy, A. V. Chechkin, A. Bodrova, and R. Metzler, Aging underdamped scaled Brownian motion: Ensemble-and time-averaged particle displacements, nonergodicity, and the failure of the overdamping approximation, Phys. Rev. E **95**, 012120 (2017).
[94] A. S. Bodrova, A. V. Chechkin, and I. M. Sokolov, Scaled Brownian motion with renewal resetting, Phys. Rev. E **100**, 012120 (2019).
[95] A. G. Cherstvy, H. Safdari, and R. Metzler, Anomalous diffusion, nonergodicity, and ageing for exponentially and logarithmically time-dependent diffusivity: Striking differences for massive versus massless particles, J. Phys. D: Appl. Phys. **54**, 195401 (2021).
[96] W. Wang, R. Metzler, and A. G. Cherstvy, Anomalous diffusion, aging, and nonergodicity of scaled Brownian motion with fractional Gaussian noise: Overview of related experimental observations and models, Phys. Chem. Chem. Phys. **24**, 18482 (2022).
[97] C. Manzo, J. A. Torreno-Pina, P. Massignan, G. J. Lapeyre Jr., M. Lewenstein, and M. F. Garcia Parajo, Weak ergodicity breaking of receptor motion in living cells stemming from random diffusivity, Phys. Rev. X **5**, 011021 (2015).
[98] R. Jain and K. L. Sebastian, Diffusion in a crowded, rearranging environment, J. Phys. Chem. B **120**, 3988 (2016).
[99] M. J. Saxton, Single-particle tracking: the distribution of diffusion coefficients, Biophys. J. **72**, 1744 (1997).

[100] W. K. Kegel and A. van Blaaderen, Direct observation of dynamical heterogeneities in colloidal hard-sphere suspensions, Science **287**, 290 (2000).
[101] E. R. Weeks, J. C. Crocker, A. C. Levitt, A. Schofield, and D. A. Weitz, Three-dimensional direct imaging of structural relaxation near the colloidal glass transition, Science **287**, 627 (2000).
[102] M. T. Valentine, P. D. Kaplan, D. Thota, J. C. Crocker, T. Gisler, R. K. Prud'homme, M. Beck, and D. A. Weitz, Investigating the microenvironments of inhomogeneous soft materials with multiple particle tracking, Phys. Rev. E **64**, 061506 (2001).
[103] T. Toyota, D. A. Head, C. F. Schmidt, and D. Mizuno, Non-Gaussian athermal fluctuations in active gels, Soft Matter **7**, 3234 (2011).
[104] N. Samanta and R. Chakrabarti, Tracer diffusion in a sea of polymers with binding zones: Mobile vs. frozen traps, Soft Matter **12**, 8554 (2016).
[105] P. Chaudhuri, L. Berthier, and W. Kob, Universal nature of particle displacements close to glass and jamming transitions, Phys. Rev. Lett. **99**, 060604 (2007).
[106] B. Wang, S. M. Anthony, S. C. Bae, and S. Granick, Anomalous yet Brownian, Proc. Natl. Acad. Sci. USA **106**, 15160 (2009).
[107] C. Beck and E. G. Cohen, Superstatistics, Physica A **322**, 267 (2003).
[108] C. Beck, Superstatistical Brownian motion, Prog. Theor. Phys. Suppl. **162**, 29 (2006).
[109] M. V. Chubynsky and G. W. Slater, Diffusing diffusivity: A model for anomalous, yet Brownian, diffusion, Phys. Rev. Lett. **113**, 098302 (2014).
[110] A. V. Chechkin, F. Seno, R. Metzler, and I. M. Sokolov, Brownian yet non-Gaussian diffusion: From superstatistics to subordination of diffusing diffusivities, Phys. Rev. X **7**, 021002 (2017).
[111] V. Sposini, A. V. Chechkin, F. Seno, G. Pagnini, and R. Metzler, Random diffusivity from stochastic equations: comparison of two models for Brownian yet non-Gaussian diffusion, New J. Phys. **20**, 043044 (2018).
[112] C. C. Maaß, N. Isert, G. Maret, and C. M. Aegerter, Experimental investigation of the freely cooling granular gas, Phys. Rev. Lett. **100**, 248001 (2008).
[113] S. Tatsumi, Y. Murayama, H. Hayakawa, and M. Sano, Experimental study on the kinetics of granular gases under microgravity, J. Fluid Mech. **641**, 521 (2009).
[114] R. D. Wildman and D. J. Parker, Coexistence of two granular temperatures in binary vibrofluidized beds, Phys. Rev. Lett. **88**, 064301 (2002).
[115] W. Wang, F. Seno, I. M. Sokolov, A. V. Chechkin, and R. Metzler, Unexpected crossovers in correlated random-diffusivity processes, New J. Phys. **22**, 083041 (2020).
[116] W. Wang, A. G. Cherstvy, A. V. Chechkin, S. Thapa, F. Seno, X. Liu, and R. Metzler, Fractional Brownian motion with random diffusivity: Emerging residual nonergodicity below the correlation time, J. Phys. A: Math. Theor. **53**, 474001 (2020).
[117] L. Berthier and G. Biroli, Theoretical perspective on the glass transition and amorphous materials, Rev. Mod. Phys. **83**, 587 (2011).
[118] R. Richert, Heterogeneous dynamics in liquids: Fluctuations in space and time, J. Phys.: Condens. Matter **14**, R703 (2002).
[119] R. Yamamoto and A. Onuki, Heterogeneous diffusion in highly supercooled liquids, Phys. Rev. Lett. **81**, 4915 (1998).
[120] W. Gotze and L. Sjogren, Relaxation processes in supercooled liquids, Rep. Prog. Phys. **55**, 241 (1992).
[121] P. S. Burada, P. Hänggi, F. Marchesoni, G. Schmid, and P. Talkner, Diffusion in confined geometries, ChemPhysChem **10**, 45 (2009).
[122] E. Syková and C. Nicholson, Diffusion in brain extracellular space, Physiol. Rev. **88**, 1277 (2008).
[123] S. Burov, J.-H. Jeon, R. Metzler, and E. Barkai, Single particle tracking in systems showing anomalous diffusion: The role of weak ergodicity breaking, Phys. Chem. Chem. Phys. **13**, 1800 (2011).
[124] M. A. dos Santos and L. M. Junior, Random diffusivity models for scaled Brownian motion, Chaos Soliton Fract. **144**, 110634 (2021).
[125] A. G. Cherstvy and R. Metzler, Anomalous diffusion in time-fluctuating non-stationary diffusivity landscapes, Phys. Chem. Chem. Phys. **18**, 23840 (2016).
[126] T. Uneyama, T. Miyaguchi, and T. Akimoto, Fluctuation analysis of time-averaged mean-square displacement for the Langevin equation with time-dependent and fluctuating diffusivity, Phys. Rev. E **92**, 032140 (2015).
[127] Y. He, S. Burov, R. Metzler, and E. Barkai, Random timescale invariant diffusion and transport coefficients, Phys. Rev. Lett. **101**, 058101 (2008).
[128] J.-H. Jeon and R. Metzler, Analysis of short subdiffusive time series: Scatter of the time-averaged mean-squared displacement, J. Phys. A: Math. Theor. **43**, 252001 (2010).
[129] A. Rahman, Correlations in the motion of atoms in liquid argon, Phys. Rev. **136**, A405 (1964).
[130] A. S. Bodrova, A. V. Chechkin, A. G. Cherstvy, and R. Metzler, Ultraslow scaled Brownian motion, New J. Phys. **17**, 063038 (2015).
[131] F. Thiel and I. M. Sokolov, Scaled Brownian motion as a mean-field model for continuous-time random walks, Phys. Rev. E **89**, 012115 (2014).
[132] A. G. Cherstvy and R. Metzler, Population splitting, trapping, and non-ergodicity in heterogeneous diffusion processes, Phys. Chem. Chem. Phys. **15**, 20220 (2013).
[133] T. J. Feder, I. Brust-Mascher, J. P. Slattery, B. Baird, and W. W. Webb, Constrained diffusion or immobile fraction on cell surfaces: A new interpretation, Biophys. J. **70**, 2767 (1996).